

# Transient Bandwidth Analysis of Photoconductive Microwave Switches Implemented in the OMEGA Pulse-Shaping System

The OMEGA laser fusion program at LLE calls for complex, temporally shaped optical pulses incident on fusion targets.<sup>1</sup> The pulse-duration and rise-time specifications of these optical pulses dictate an electrical pulse-shaping system bandwidth of approximately 0.1 to 10 GHz. The optical pulses are created by imprinting an electrical equivalent of the desired optical envelope onto an optical square pulse, using an integrated-optics Mach-Zehnder interferometric electro-optic modulator as shown in Fig. 76.20. The electrical pulse shape is generated by the reflection of an electrical square pulse from a distributed variable-impedance microstrip transmission line. The electrical square pulse is generated by illuminating a photoconductive semiconducting (PCS) switch in a series-gap configuration, which discharges a microstrip transmission line charged with a dc voltage. Assuming the PCS switch is saturated by the illumination, the rise time of the electrical pulse corresponds to the rise time of the optical illumination trigger

pulse, and the switch conductivity remains roughly constant for the duration of the electrical pulse. The fall time is computed by convolving the rise time with the reflection impulse response of the second, unilluminated switch.<sup>2</sup> The resulting propagating square pulse has an amplitude of half the dc voltage and a duration of twice the charge-line's round-trip time.<sup>3</sup>

Measurements of the shaped electrical signal before and after the PCS switches, as shown in Fig. 76.21, indicate that the frequency response of the shaped laser pulse is strongly limited by the transmission of the shaped electrical pulse through the PCS switches. Time-gated microwave measurements of the switch attenuation did not reveal the source of the switch's bandwidth limitations.<sup>4</sup> In this latter case, however, the optical illumination conditions were significantly different from the actual OMEGA operating conditions, and the measurements were performed using a simple time-windowed,

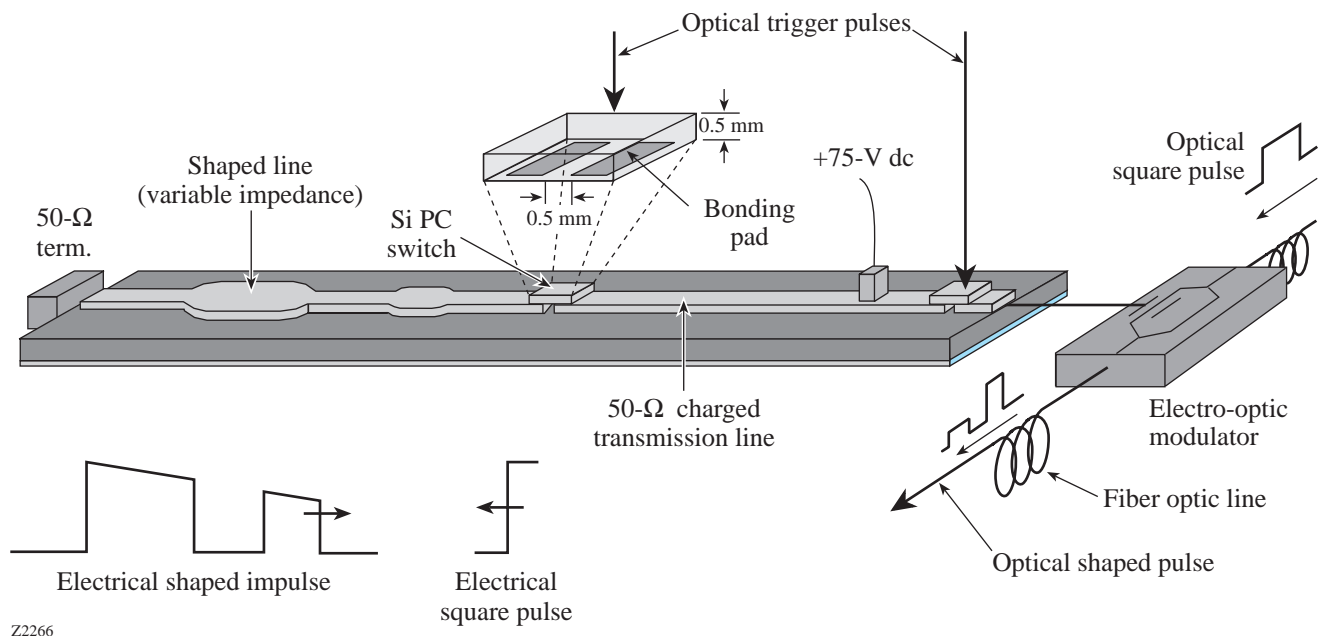


Figure 76.20  
The microwave signal reflected from the shaped variable impedance line must pass through two PCS switches before reaching the electro-optic modulator.

power-detection technique. Also, phase/dispersion variations and decay of the PCS switch transmission within the measurement time window could not be detected with this technique. These limitations motivated the design and implementation of the improved measurement scheme described in this article.

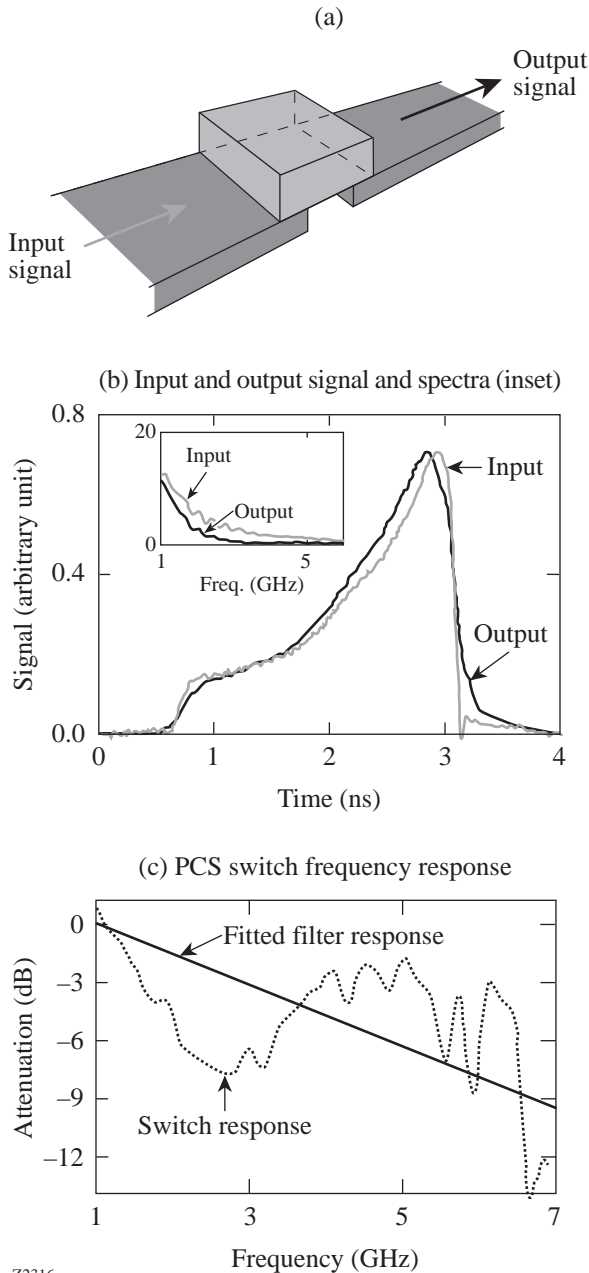


Figure 76.21 The PCS switch, microstrip line, and input and output signals are shown graphically in (a). These signals were (b) measured and their spectra found (inset). The (c) switch response was computed by a ratio of the spectra and compared to a single-pole low-pass filter.

PCS switches, unlike conventional diode or transistor microwave switches, do not operate in a steady-state “on/closed” condition. After optical illumination, the carrier recombination dynamics cause the switch transmission to decay to an “off/open” state. For example, the PCS switches used on OMEGA are typically driven to their highest (saturated) charge-carrier density by a 500-ps, 100- $\mu$ J optical pulse. After illumination, the carrier density decays monotonically, meaning that the PCS switch’s on-state is transient in nature since it depends on the carrier recombination dynamics. This imposes requirements beyond the capabilities of conventional microwave test equipment (e.g., network analyzers, modulation analyzers): PCS switches as implemented in the OMEGA pulse-shaping system cannot be modeled as exclusively filters or modulators. The modulator model breaks down because PCS switches transmit signals with a bandwidth comparable to the transmission bandwidth of the switch, and they don’t fit the filter model well because of their time-varying properties. Note that due to thermal damage issues at the metal–semiconductor (soldered-contact) interface, cw optical illumination for the purpose of creating a time-invariant device in the saturated regime is not possible.<sup>5</sup> This means that it is necessary to use transmission equations for a linear device that are more general than those for filters and modulators and to develop a measurement system capable of measuring a generalized transmission function.

We describe a method for measuring the transient complex (amplitude and phase) frequency response of a microwave device, and we give results for PCS switch measurements. These measurements were performed with PCS switch excitation conditions identical to those used on OMEGA, and over temporal durations and frequency ranges of interest to OMEGA pulse-shaping experiments. With this system, microwave devices whose transient bandwidths were previously only approximated can now be characterized and compared with a more general, multiport microwave device theory. This measurement scheme is compatible with triggerable microwave devices that have a deterministic time evolution; other examples aside from photoconductive devices are amplifier and active filter turn-on/turn-off transients and atmospheric multipath fading due to relative antenna motion.

**Theoretical Background**

From a linear-system viewpoint, the relationship between the input and output voltage signals of the device under test (DUT) shown in Fig. 76.22(a) is

$$V_n(\omega) = S(\omega) \cdot V_m(\omega), \tag{1}$$

where  $V_m(\omega)$  and  $V_n(\omega)$  are the total voltages across ports  $m$  and  $n$  and  $S(\omega)$  is the DUT (filter) frequency response. Equation (1) can be Fourier transformed to

$$v_n(t) = \int_{\tau=-\infty}^{\tau=\infty} h(t-\tau) \cdot v_m(\tau) d\tau, \quad (2)$$

where  $v_m(t)$  and  $v_n(t)$  are the total instantaneous voltage signals and  $h(t)$  is the impulse response.

Measurements of microwave devices conventionally involve either scalar or vector network analysis of scattering or  $S$  parameters, where  $a_n(\omega)$  and  $b_n(\omega)$  are the incident and scattered signals from a port  $n$ , which has a characteristic impedance  $Z_0$ , also shown in Fig. 76.22.<sup>6</sup> These microwave signals  $a$  and  $b$  are related to the total voltage across the port by the incident and reflected voltages  $V^+$  and  $V^-$ :

$$a = \frac{V^+}{\sqrt{Z_0}}, \quad b = \frac{V^-}{\sqrt{Z_0}} \quad (3)$$

and are related to each other (for a two-port DUT) by the relationship

$$\begin{bmatrix} b_1 \\ b_2 \end{bmatrix} = \begin{bmatrix} S_{11} & S_{12} \\ S_{21} & S_{22} \end{bmatrix} \begin{bmatrix} a_1 \\ a_2 \end{bmatrix}. \quad (4)$$

Since the PCS switches operate in the transmission mode, we will focus on the  $S_{21}$  parameter. The  $S_{21}$  parameter relates the signal transmitted from port 2 (output) to the signal incident on port 1 (input) in the frequency domain; this relation is similar to Eq. (1) and is given by

$$b_2(\omega) = S_{21}(\omega) \cdot a_1(\omega). \quad (5)$$

The transmission parameter  $S_{21}$  is defined in the spectral domain because of the assumed linear time invariance of the DUT. The assumption of a linear time-invariant (LTI) device is only appropriate, however, when the DUT response approaches an ideal filter (i.e., does not vary in time).

A linear device such as an ideal amplitude or phase modulator is not time invariant. Modulators are typically measured with spectrum or modulation analyzers in the linear small-signal regime with narrow-band (cw) input signals, so that the assumption of an infinite-bandwidth ideal modulator introduces negligible error. The equations characterizing a modulator's input-output relationship is then exactly complementary to Eqs. (1) and (2):

$$v_n(t) = k(t) \cdot v_m(t) \quad (6)$$

$$V_n(\omega) = \int_{\xi=-\infty}^{\xi=\infty} K(\omega-\xi) \cdot V_m(\xi) d\xi, \quad (7)$$

where  $k(t)$  and  $K(\omega)$  are the modulation function and its transform.<sup>7</sup>

If a linear device cannot be approximated as either time invariant or as having infinite bandwidth, then none of the above equations is appropriate. Test systems that are based on these equations (such as spectrum, modulation, and network analyzers) are unable to measure the transfer function of such a device; therefore, a more general input-output relationship has been developed. This was done by recognizing that any linear device can be characterized by the generalized form of the filter and modulator Eqs. (2) and (7):

$$v_n(t) = \int_{\omega=-\infty}^{\omega=\infty} G(t,\omega) \cdot V_m(\omega) d\omega, \quad (8)$$

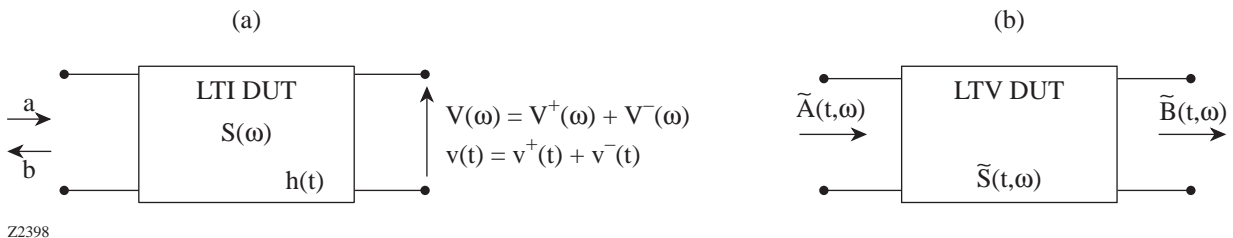


Figure 76.22 (a) Conventional LTI (filter) two-port microwave devices use a scattering matrix to define input-output relationships between the signals, while (b) LTV microwave devices relate input to output via a more general  $\tilde{S}(t,\omega)$  matrix.

where  $G(t, \omega)$  is the (more general) input–output relation, now a function of both time and frequency.<sup>8</sup> This function  $G(t, \omega)$  has a simple extension to conventional microwave measurements if it is viewed as a generalized  $S(\omega)$  parameter and renamed  $\tilde{S}(t, \omega)$ , as shown in Fig. 76.22(b). The input–output transmission function is similar to Eq. (5):

$$\tilde{B}_2(t; \omega) = \tilde{S}_{21}(t, \omega) \cdot \tilde{A}_1(t; \omega), \quad (9)$$

where  $\tilde{A}$  and  $\tilde{B}$  are joint time–frequency distributions of one-dimensional functions (indicated by the semicolon between the variables) related to  $v^+$  and  $v^-$  by the Wigner time–frequency (WTF) distribution<sup>9</sup>

$$\tilde{A}(t; \omega) = \frac{1}{Z_0} \int_{-\infty}^{\infty} v^+(t + \tau/2) v^{+*}(t - \tau/2) e^{-j\omega\tau} d\tau, \quad (10)$$

and  $\tilde{B}$  is defined similarly for  $v^-$ .

This input–output relationship of Eq. (9) is simpler than the integral function of Eq. (8) and has the further advantage that in the microwave regime the signals  $a$  and  $b$  are more easily measured than the total transmission-line voltages  $V_m(\omega)$  and  $v_n(t)$ . Any  $\tilde{S}$  parameter can be determined from Eq. (9) and from measurements of the input and output microwave signals at the appropriate ports. For example, in a two-port microwave device such as a PCS switch, if the microwave signal is incident on port 1 and the response measured at port 2, the  $\tilde{S}_{21}$  parameter can be determined by dividing the WTF distribution of the output (port 2) signal by the WTF distribution of the input (port 1) signal. Comparing Eqs. (9), (1), and (5), the parameter  $\tilde{S}_{21}(t, \omega)$  can be seen as a time-varying frequency response  $S(\omega)$ .

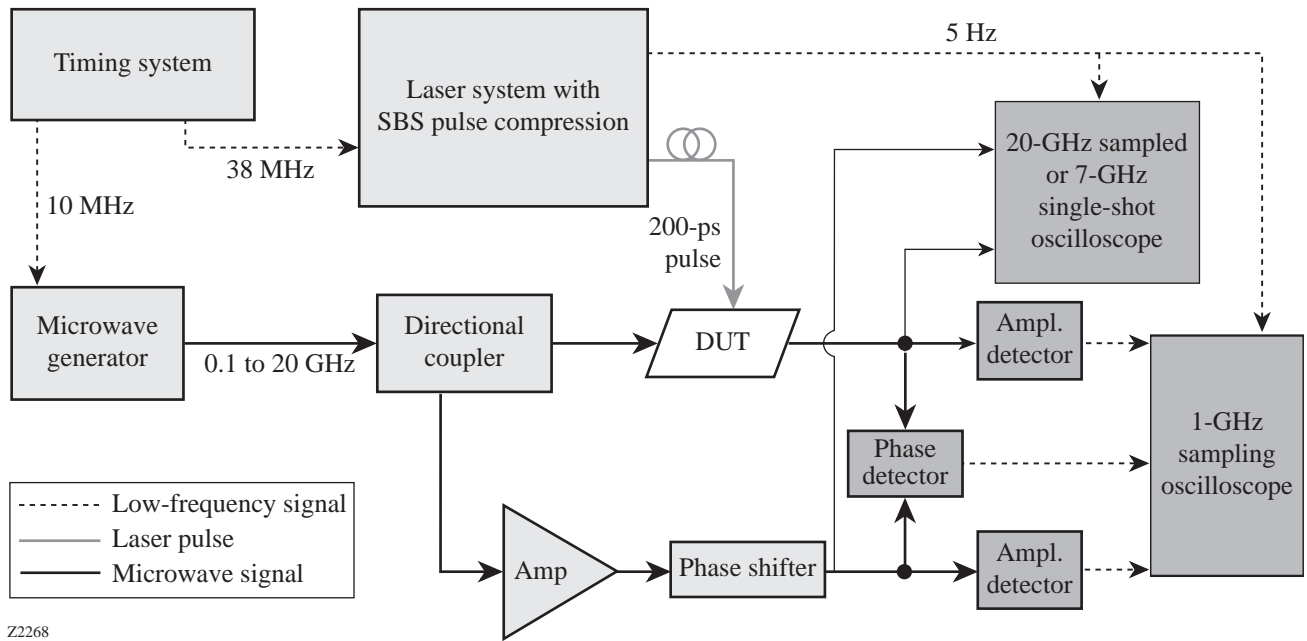
Note that  $\tilde{S}$  is the (complex) time-varying frequency response of the microwave device and is to be distinguished from the time-varying spectrum of a signal  $\tilde{A}$ , a joint time–frequency distribution generated from a one-dimensional (complex) signal by Eq. (10). To make this difference between  $\tilde{A}$  and  $\tilde{S}$  apparent, one can Fourier transform  $\tilde{S}$  in the second variable ( $\omega$  to  $\tau$ ), which results in  $\tilde{S}(t, \tau)$ . A magnitude surface plot of this two-dimensional function shows the temporal change of the impulse response “ $h(\tau)$ ” with time  $t$ . In contrast, transforming  $\tilde{A}$  in either variable will result in a surface plot of a one-dimensional function multiplied by itself along each axis, i.e., if  $\tilde{A}(t; \omega)$  was Fourier transformed in the second variable ( $\omega$  to  $\tau$ ), the resulting function  $\tilde{A}(t; \tau)$  would by definition be proportional to  $v^+(t) \cdot v^+(\tau)$ . This is simply  $v^+(t)$

multiplied by itself in the second, dummy variable  $\tau$  and therefore not a function of two independent variables, as  $\tilde{S}(t, \tau)$  is. Thus, the time-varying bandwidth  $\tilde{S}$  of a device is distinct from the time-varying spectrum of a signal  $\tilde{A}$ .<sup>10,11</sup>

### Experimental Design

The system we created to measure the time and frequency variations of the switch’s transfer function is based on a microwave interferometric measurement and is shown in block-diagram form in Fig. 76.23. The DUT for which we measure the two-dimensional transfer function  $\tilde{S}(t, \omega)$  is shown at the center of the figure (in our case, a PCS switch). The DUT is triggered (in our case, by a laser pulse), causing a single-frequency microwave signal of known power and phase from the microwave generator to propagate through the DUT and also through a separate, parallel reference arm consisting of an amplifier and a phase shifter. The two arms, after splitting at the directional coupler, are recombined and compared to one another in amplitude (at the diode detectors) and phase (at the mixer/phase detector). Alternatively, the signal from each arm can be measured directly by an oscilloscope of sufficiently high bandwidth and subsequently compared. Both measurements are shown in Fig. 76.23. The timing system synchronizes the triggering of the DUT with the phase of the microwave signal incident on it, so that each trigger occurs at the same phase of the microwave signal. This allows sampling oscilloscope measurements, which improves the measurement resolution over single-shot digitizing oscilloscopes.

The signal-measurement process proceeds in the following step-and-dwell manner: The microwave generator is set to a single given frequency of known phase and amplitude. The DUT is then triggered, and the evolution of the transmitted signal is measured and compared with the reference arm signal for the temporal duration of interest. The microwave generator then steps to the next microwave frequency, and the process repeats for the range of frequencies of interest. The recorded data is then reduced to two sets of complex (amplitude and phase), two-dimensional arrays of incident and transmitted signals corresponding to  $\tilde{A}$  and  $\tilde{B}$ . Using Eq. (9) we calculate the transfer function  $\tilde{S}(t, \omega)$ , which can then be analyzed for bandwidth and modulation features. For a PCS switch, the transfer function is expected to show an exponentially decaying modulation due to carrier recombination and a (possibly changing) bandwidth, which can be modeled by a lumped-element circuit consisting, in general, of a time-changing reactance and a time-changing resistance. The values of these elements can then be associated with switch properties such as carrier lifetime, non-ohmic contacts, thickness and gap length,



Z2268

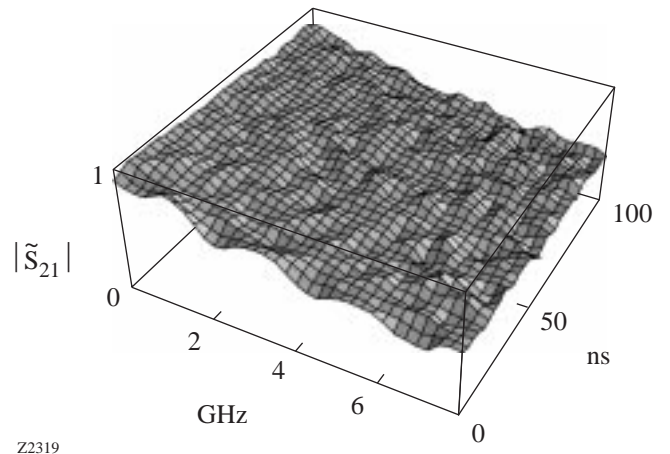
Figure 76.23  
Signal flow of system capable of analyzing transient-bandwidth devices.

and the bandwidth of the switch can be optimized by appropriately modifying these switch properties. For example, the metal–semiconductor interface can be made Schottky or ohmic-like by selective ion implantation and dopant diffusion, which affects carrier recombination, surface velocity, trapping states, and contact resistance. Switch thickness and switch-gap width and length will affect capacitive coupling and series resistance and should be selected so as to minimize the switch RC time constant and maximize photon absorption.

### Experimental Results

A representative magnitude plot of the two-dimensional transfer function  $\tilde{S}(t, \omega)$  of a PCS switch is shown in Fig. 76.24. As explained in the **Theoretical Background** section,  $\tilde{S}(t, \omega)$  is necessary to describe the transmission response of a PCS switch [ $S(\omega)$  is inadequate] because the switch modulates a signal whose spectral content is comparable to its bandwidth. Features of the transfer function, such as the conductive carrier decay along the temporal axis and frequency-dependent attenuation along the spectral axis due to bandwidth limitations, are readily observed. By numerically fitting a linear lumped-element model having both filtering and modulating components to the measured transfer function, values of various microwave components can be extracted. The fitted model,

shown in Fig. 76.25, is a simple low-pass filter in series with an exponentially decaying resistive element. The switch’s 3-dB bandwidth is approximately 5 GHz, which agrees well with the observed bandwidth loss of shaped pulses propagating through the OMEGA pulse-shaping system (Fig. 76.26).



Z2319

Figure 76.24  
Measured  $\tilde{S}_{21}(t, \omega)$  shows carrier decay along the temporal axis and bandwidth limitations along the spectral axis.

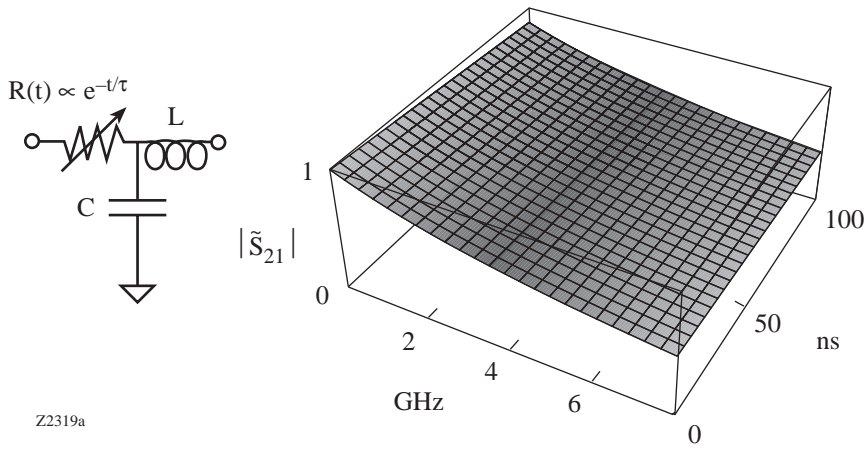
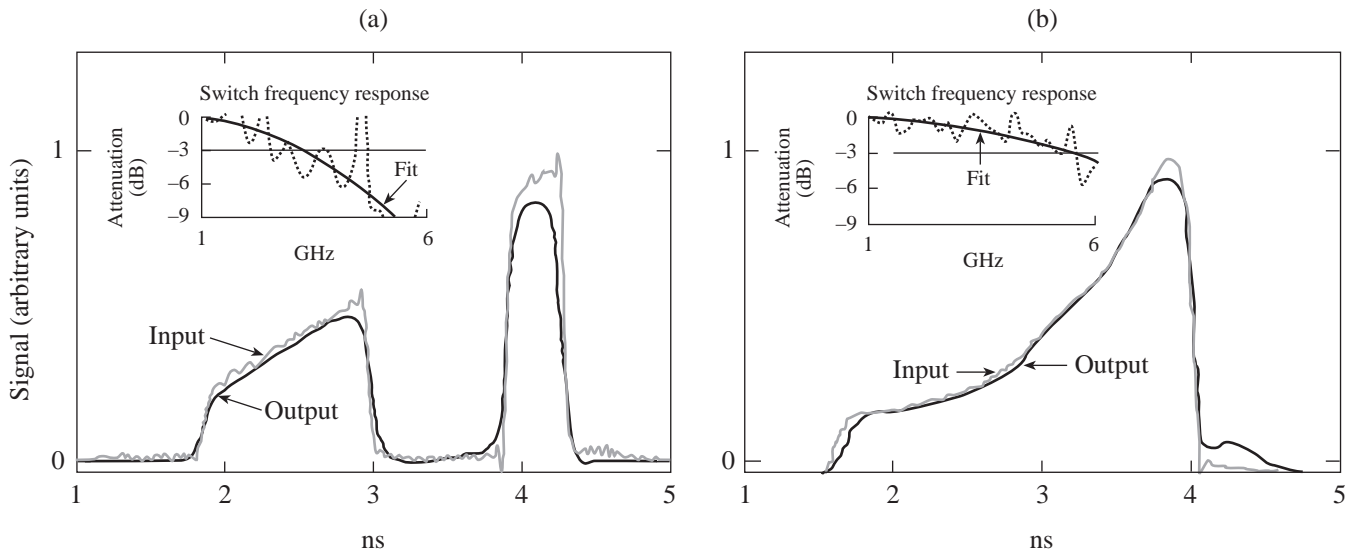


Figure 76.25 Modeled  $\tilde{S}_{21}(t, \omega)$  accurately fits an exponentially decaying resistance in series with a low-pass filter to the measured data.



Z2320

Figure 76.26

By optimizing switch parameters, transmission bandwidth on OMEGA pulse shaping has been improved from (a) mid-1995, the beginning of OMEGA's pulse shaping, to (b) early 1998.

**Conclusions**

Measurements of optical and electrical temporal pulse shapes at different locations in our pulse-shaping system indicate that the primary bandwidth limitations occur during transmission of our electrical pulse shapes through the PCS switches. When pulse shaping was first implemented on OMEGA, the measured attenuation at 10 GHz (corresponding to 30-ps pulse rise- and fall-times) was more than 12 dB through the switch, and the 3-dB bandwidth was near 3 GHz. This frequency response is significantly worse than the other components in the pulse-shaping system: e.g., microstrip trans-

mission line, connectors, and electro-optic modulator. Modeling of photoconductive switches<sup>12</sup> indicates that a much larger bandwidth is theoretically possible; thus, efforts were taken to isolate and comprehensively measure the microwave transmission bandwidth of our PCS switches. This characterization made possible the systematic optimization of the many parameters of the switch, such as gap length, microwave skin depth versus optical absorption depth, and metal-semiconductor contact preparation. Since conventional network analyzers were incapable of determining the bandwidth of a device that varied in time, a measurement system was designed and built

tailored to such time-varying devices. This measurement system allowed determination of the relationship between the properties of the switch and its frequency response characteristics. By improving the physical switch properties, the 3-dB bandwidth of the OMEGA pulse-shaping PCS switches has been increased to over 5 GHz. The full bandwidth of the implemented PCS switches is now as broad as the next-most-limiting device in the pulse-shaping system (believed to be the electro-optic modulator) and is sufficient for current OMEGA optical-pulse-shape requirements.

#### ACKNOWLEDGMENT

This work was supported by the U.S. Department of Energy Office of Inertial Confinement Fusion under Cooperative Agreement No. DE-FC03-92SF19460 and the University of Rochester. The support of DOE does not constitute an endorsement by DOE of the views expressed in this article. The author also acknowledges the support of the Frank Horton Graduate Fellowship Program.

#### REFERENCES

1. M. D. Skeldon, A. Okishev, S. A. Letzring, W. R. Donaldson, K. Green, W. Seka, and L. Fuller, in *Optically Activated Switching IV*, edited by W. R. Donaldson (SPIE, Bellingham, WA, 1994), Vol. 2343, pp. 94–98.
2. G. H. Owyang, *Foundations for Microwave Circuits* (Springer-Verlag, New York, 1989).
3. S. C. Burkhart and R. B. Wilcox, *IEEE Trans. Microwave Theory Tech.* **38**, 1514 (1990).
4. K. Green, W. R. Donaldson, R. Sobolewski, A. Okishev, M. D. Skeldon, S. A. Letzring, and W. Seka, in *First Annual International Conference on Solid State Lasers for Application to Inertial Confinement Fusion*, edited by M. André and H. T. Powell (SPIE, Bellingham, WA, 1995), Vol. 2633, pp. 615–621.
5. W. C. Nunnally, in *High-Power Optically Activated Solid-State Switches*, edited by A. Rosen and F. Zutavern (Artech House, Boston, 1994), pp. 29–42.
6. K. Kurokawa, *IEEE Trans. Microw. Theory Tech.* **MTT-13**, 194 (1965).
7. H. D'Angelo, *Linear Time-Varying Systems: Analysis and Synthesis*, The Allyn and Bacon Series in Electrical Engineering (Allyn and Bacon, Boston, 1970).
8. L. A. Zadeh, *J. Appl. Phys.* **21**, 642 (1950).
9. M. A. Poletti, *J. Audio Eng. Soc.* **36**, 457 (1988).
10. D. J. Kane and R. Trebino, *Opt. Lett.* **18**, 823 (1993).
11. F. T. S. Yu and G. Lu, *Appl. Opt.* **33**, 5262 (1994).
12. S. S. Gevorgian, *IEE Proc. J, Optoelectron.* **139**, 153 (1992).

